The Astrophysical Journal, 632:1176–1183, 2005 October 20

MOVING MAGNETIC FEATURES AS PROLONGATION OF PENUMBRAL FILAMENTS

A. Sainz Dalda[1]
Télescope Héliographique pour l'Etude du Magnétisme et des Instabilités Solaires (THÉMIS),
Instituto de Astrofísica de Canarias, 38205 La Laguna, Tenerife, Spain; asainz@themis.iac.es

and

V. Martínez Pillet
Instituto de Astrofísica de Canarias, 38205 La Laguna, Tenerife, Spain; vmp@iac.es
Received 2005 April 4; accepted 2005 June 25

ABSTRACT

A sequence of 633 high spatial resolution magnetograms and continuum images from *SOHO* MDI of NOAA AR 0330 is used to study moving magnetic feature (MMF) activity in the moat surrounding a mature leader sunspot. The time-averaged frame shows that the moat region is covered by a magnetic field that exhibits the same polarity distribution as that observed in the penumbra. The moat field displays the true polarity of the spot in the sector where the penumbra displays it. Similarly, on the side where the penumbra shows a polarity opposite the true one (due to projection effects after the so-called apparent neutral line), the moat field also displays a polarity opposite the true one. This is only compatible with a moat field that is horizontal almost everywhere, as in the outer penumbra. Indeed, this horizontal moat field is seen to be physically connected with the penumbra. This connection is made evident when analyzing the individual structures detected in the averaged images, which we call moat filaments. The filaments stretch out for 12″ in the moat and can be traced back into the penumbra. The observed polarity distribution along them is only compatible with mean inclinations in the range of 80°–90°. Inside the spot, these filaments are linked to the more horizontal magnetic field component that is thought to carry a large part of the Evershed flow. Several bipolar MMFs are seen to originate inside the penumbra and cross the sunspot outer boundary to enter the moat region, following the paths outlined by the moat filaments. These results are discussed in the frame of our current theoretical understanding of the Evershed flow and MMF activity.

Subject headings: Sun: atmospheric motions — Sun: magnetic fields — sunspots

Online material: mpeg animations

1. INTRODUCTION

During the last decade our understanding of the structure of penumbral magnetic fields has increased enormously. Line-of-sight (LOS) magnetograms obtained by Title et al. (1993) showed that there exist fluctuations of the magnetic field inclination as large as ±18°, at a spatial resolution of 1″. They referred to these structures as the fluted penumbral magnetic field. Lites et al. (1993), using Advanced Stokes Polarimeter (ASP) data, found that, in fact, the fluctuations of the magnetic field occurred simultaneously in both field strength and inclination. The two magnitudes were strongly correlated in the sense that the less inclined (more vertical) structures, which they named spines, had stronger field strengths, while the more horizontal filaments (intraspines) had weaker fields. These structures were further elaborated into a model in which intraspine field lines constitute almost horizontal flux tubes wrapped around by a background field (the spines) in the so-called uncombed penumbral magnetic field by Solanki & Montavon (1993). In addition, the well-known Evershed flow observed in the penumbra was found to be concentrated in the horizontal field lines (i.e., the penumbral flux tubes) according to all these works. Another important ingredient of our understanding of the penumbral magnetic fields came from the results obtained by Westendorp Plaza et al. (1997), who showed that near the outer penumbral boundary and in the lower parts of the atmosphere, one could find field lines carrying significant amounts of the Evershed flow that were directed downward, back into the photosphere. These results have been verified by several authors (Schlichenmaier & Schmidt 2000). Indeed, infrared observations (from the Tenerife Infrared Polarimeter [TIP]) analyzed in similar ways to the ASP data (del Toro Iniesta et al. 2001; Bellot Rubio et al. 2004) showed that these returning field lines are also found in the mid-penumbra. In particular, Bellot Rubio et al. (2004) have found that the tubes carrying the Evershed flow are horizontal at a radius of 0.8 times the sunspot radius, while at the outer penumbral boundary (as defined in continuum intensity images) they have a mean inclination of 115°. By contrast, the spine (vertical) component has, at the same boundary, an inclination of 60°. All in all, this constitutes the first qualitative and quantitative model at hand of the magnetic structure in the penumbra (recent reviews have been provided by Bellot Rubio 2003; Solanki 2003; Thomas & Weiss 2004).

The inclination of the mean magnetic field at the penumbral boundary reaches 70°–80° (Martínez Pillet 1997; Bellot Rubio 2003). This has the well-known implication that spots observed outside the disk center show an apparent neutral line (a region where the line-of-sight magnetic field $B_{\rm LOS}$ is 0 and that divides the spot in two areas with opposite polarities). For round sunspots, this neutral line is perpendicular to the radius vector connecting the Sun's disk center and the spot. The neutral line normally falls in the so-called limb-side penumbra, i.e., the penumbra closest to the limb (if the spot is too close to the solar limb, the neutral line can enter the umbra). Correspondingly, the penumbra that is closest to the disk center is called the center-side penumbra. This penumbral side always displays the true

[1] Operator of the THÉMIS telescope, Observatorio del Teide, Tenerife, Spain.

polarity of the spot, whereas the limb-side penumbra only displays it in between the umbra and the neutral line. Beyond the neutral line, the limb-side penumbra displays the opposite polarity. Note that in a two-component penumbral model with different inclinations, one expects to see two different apparent neutral lines. The more horizontal component will show a neutral line lying closer to the umbra, while the more vertical component will display a neutral line closer to the penumbral boundary. As a result, a corrugated neutral line lying somewhere in between these two neutral lines is expected. The precise location depends on the weightings made by each of the two components (this corrugated neutral line has been observed by, e.g., Title et al. 1993).

As pointed out above, the more horizontal component of the penumbral magnetic field turns back down into the deeper photospheric layers already inside the penumbra. What happens to this penumbral component beyond that point is not clear. The continuum intensity and velocity flow boundaries defining the end of the spot are rather sharp, supporting the idea of an outer boundary where the spot would end. This fact is not so evident from a magnetic point of view. Sunspots have long been known to be surrounded by a conspicuous bipolar outflow called moving magnetic feature (MMF) activity (see Sheeley 1969). Harvey & Harvey (1973) proposed that MMFs constitute fully detached field lines from the spot during its decay. These detached field lines would be carried out by the so-called moat flow surrounding the spot. This moat flow is thought to be related to some form of supergranular cell that would surround all mature sunspots (see Meyer et al. 1974). However, Martínez Pillet (2002) has recently found that the net flux generated in this moat exceeds the flux losses from the spot by at least a factor of 3–4, strongly suggesting that MMF activity is not caused by phenomena related to sunspot decay. Indeed, Martínez Pillet (2002), Thomas et al. (2002), and Schlichenmaier (2002) have suggested that MMF activity could be linked to the continuity of the horizontal component of the penumbra carrying the Evershed flow. Some theoretical results in this direction have been obtained in numerical simulations (Schlichenmaier 2002; Thomas et al. 2002). From an observational point of view, only Lee (1992) suggested that the MMFs originate more frequently near the end of dark penumbral fibrils but provided no real evidence of a link between them and the penumbral field lines.

In a comprehensive review of MMF activity, Shine & Title (2001) showed that a temporally averaged image made in the core of the Ca II K line shows MMF activity as bright radially oriented paths surrounding the spot. These structures are reminiscent of the filaments in the penumbra and suggest a link between them, but flux detached from the spot carried by a radially directed moat flow would also generate similar paths. In this paper, we show that by similarly averaging *Solar and Heliospheric Observatory* (*SOHO*) Michelson Doppler Imager (MDI) magnetograms over 10 hr, we are able to trace magnetic filaments from the outer part of the moat well into the penumbra, where they become magnetic filaments similar to those detected by Title et al. (1993). Along some of these moat filaments, bipolar MMFs are seen to occur during the time interval analyzed. The results presented here establish a clear connection between penumbral field lines, magnetic filaments in the moat region, and the bipolar MMF activity observed all around sunspots.

2. DATA PROCESSING

The NOAA AR 0330 was observed by *SOHO* MDI (Scherrer et al. 1995) in its high-resolution observing mode with a spatial and temporal sampling of 0.″60 and 1 minute, respectively. All the available LOS magnetograms and continuum images of this active region have been processed, from which we select the longest nonstop interval. It starts on 2003 April 9 at 14:05 UT and finishes on 2003 April 10 at 00:49 UT. One bad image was removed and 13 images are missing from this interval. The final data set includes 633 frames. The μ-value of NOAA AR 0330 is 0.984, which corresponds to a heliocentric angle of 10°. Note that in this case, field lines in the central part of the limb-side penumbra and inclined 80° with respect to the local vertical will show no LOS component of the magnetic field, marking the location of the observed neutral line.

We are interested in concentrating on the temporal evolution of the prominent MMF activity observed around this sunspot. To this end, it is crucial that the sunspot is always perfectly centered in all the frames of our data set. We follow the transit of the sunspot through the *SOHO* MDI high-resolution area, selecting a square region of $180.''6 \times 180.''6$, taking into account solar rotation and correcting for border effects. All magnetograms are further co-aligned by searching for the maximum of their correlation with respect to a reference frame and displacing them by Fourier interpolation. The continuum images are treated in the same way, and the mean umbral and penumbral contours are defined from the average image obtained from the 633 continuum frames. The mean umbra-penumbra and penumbra-photosphere contours are interpolated at intensities of 0.62 and 0.93, respectively. These contours provide a reference for the traditional photometric boundaries of the spot. In addition to the mean contours, we also make use of the instantaneous contours from individual continuum snapshots.

Figure 1 depicts individual continuum and magnetogram images extracted from the animations included in the online material. The images display the instantaneous contours of the umbra and penumbra. The magnetogram (Fig. 1*b*, scaled to $\pm$100 G) clearly shows the bipolar MMF activity outside the penumbral boundary. On the limb-side penumbra (limb is toward the top [north] of each image), one observes the corrugated neutral line as the gray region that is intermittently crossed by white filaments. Occasionally, they reach the outer penumbral boundary. As explained in § 1, the corrugated neutral line can be understood in terms of a two-component model with different inclinations. First, note that for this relatively high μ-value, the more vertical component (with inclinations no larger than 60°) never shows a neutral line. On the other hand, the more horizontal penumbral component, with inclinations that exceed 80°, shows an apparent neutral line and even opposite polarity. When we see the limb-side penumbra crossed by white filaments, it is clear that it corresponds to pixels with a higher contribution from the more vertical component. The black and gray regions would correspond to pixels dominated by the more horizontal component. Note that, as pointed out in § 1, this component is thought to carry the Evershed flow.

With all of the 633 frames analogous to those in Figure 1, we generate two animations of the evolution of the leading sunspot of NOAA AR 0330. They can be found in the electronic edition of this work. The animations display the instantaneous contours of the umbra and penumbra.

3. RESULTS

The first animation is made with the continuum intensity frames and shows the fluctuations in the location of the instantaneous penumbral boundary during the studied interval. The second one is a magnetogram animation (scaled to $\pm$100 G) that allows a detailed view of the MMF activity surrounding the spot. The instantaneous photometric contours are overlaid on this

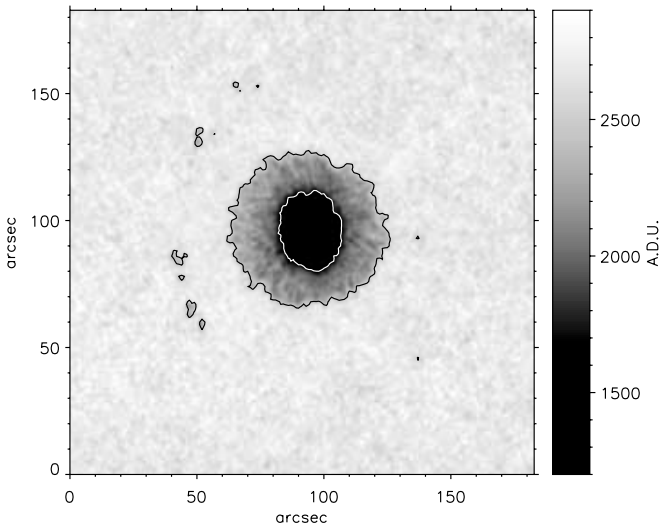

FIG. 1*a*

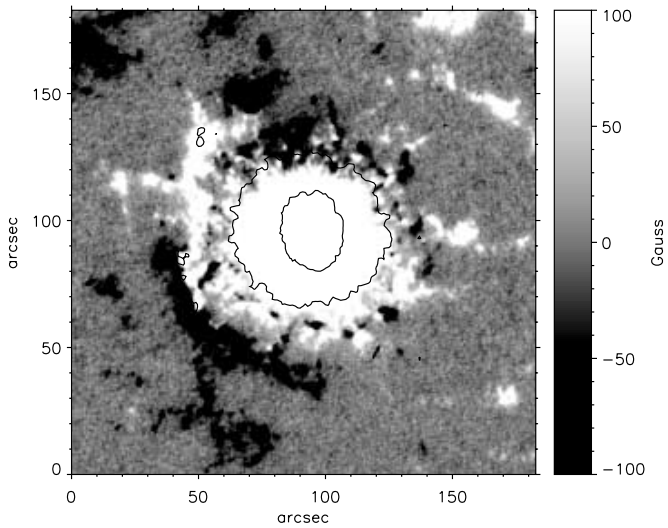

FIG. 1*b*

FIG. 1.—(*a*) Individual intensity image with the instantaneous umbral and penumbral contours overlaid. (*b*) Corresponding magnetogram (scaled between ±100 G; positive polarity is coded white, while negative polarity is coded black). The images correspond to snapshots 23 for the continuum intensity and 25 for the magnetogram of their respective data sets. [*This figure is available as two mpeg files in the electronic edition of the Journal.*]

animation as well. In the second animation, the MMF activity with all three components found by Shine & Title (2001) can be identified: bipolar structures, unipolar structures with the same polarity as the spot, and fast-moving unipolar structures with opposite polarity. The animation shows a fourth component of the MMF activity, which corresponds to an almost continuous swell of outward-moving flux that cannot be described as isolated structures but appears to be instead a large-scale process taking place everywhere in the moat. The most remarkable property of this magnetic swell is that it has negative polarity in the limb side of the moat but positive polarity in the center side of the moat. This clearly points toward a process occurring in almost horizontal field lines filling a large part of the moat.

In order to search for the presence of magnetic links between the penumbra and the MMF activity, following Shine & Title (2001) we average in time the resulting data set. The average is made in two ways: (1) using the absolute value of the individual magnetograms, giving rise to what we refer to as $\langle|\Phi|\rangle$,[2] and (2) using the magnetograms with their true sign, producing $\langle\Phi\rangle$. The brackets refer to temporal average.

The averaged images of the absolute value and true sign magnetograms are given in the left and right panels of Figure 2, respectively. Interestingly, they both show filamentary structures in the moat region, all around the spot. These moat filaments are analogous to those shown by Shine & Title (2001). However, and most importantly, they are now seen as structures that originate inside the penumbra. The visibility of the filaments is different on the limb and center sunspot sides and depends on the scaling used for the images. In the absolute value image (*left*) a scaling between 0 and 200 G is used. This allows us to see two filaments (*arrows*) protruding into the moat region from the penumbra. The center-side field lines, being more aligned with the

[2] While we use the term "magnetic field" when referring to the MDI measurements, the use of Φ is selected to acknowledge the magnetic flux nature of these measurements.

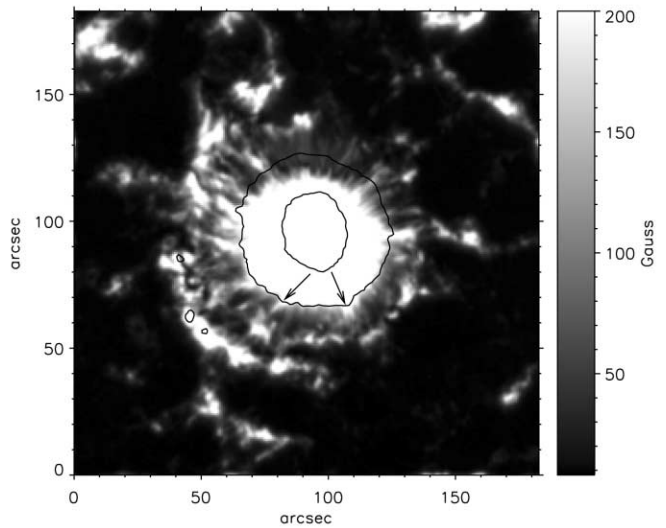

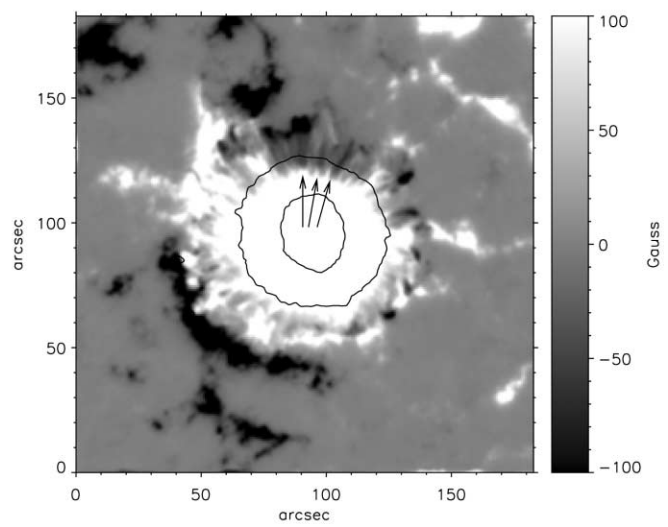

FIG. 2.—Average of the absolute value (*left*) and true sign (*right*) magnetograms with the mean umbral and penumbral contours overlaid. The left panel (absolute value average, $\langle|\Phi|\rangle$) is scaled between 0 and 200 G, while the right panel (true sign average, $\langle\Phi\rangle$) is scaled between ±100 G. The moat filaments are presented all around the sunspot; the arrows point out two examples in the center-side moat (*left*) and three in the limb-side moat (*right*).

line of sight as compared to the limb side, produce stronger magnetogram signals. The limb-side penumbra is hardly seen with this scaling. The true sign image (*right*), scaled to ± 100 G, provides a better view of the limb-side penumbra. We find three regions (*arrows*) where filaments start inside the penumbra and cross into the moat region. There are other cases of similar filaments (in the limb and center sides), but they are less prominent. All limb-side filaments show negative polarity in the moat region. Indeed, the penumbral neutral line on the limb side defines a sector over which parts of the penumbra and moat fields are of negative polarity. The rest of the moat, mostly corresponding to the center side, is largely dominated (as seen in the true sign image, *right*) by positive polarity structures. A separation in the true sign average image between negative and positive polarity sides in agreement with the location of the penumbra neutral line can only be generated by a *predominantly horizontal moat magnetic field*. MMF activity, with its different components, cannot give rise to such a configuration. MMF activity can be of two types (following Shine & Title 2001), bipolar or monopolar. Bipolar structures that follow a radial path have a strong tendency to cancel out in the true sign average image $\langle \Phi \rangle$ and would not contribute to it (although they do in the absolute value image $\langle |\Phi| \rangle$, see below). The cancellation would be perfect if, as suggested by almost all MMF models, the two polarities corresponded to successive emergences and immersions of the same field lines. In the case of monopolar MMFs, they would contribute to both average images of Figure 2. But monopolar MMFs (say, as resulting from the sunspot decay process with the spot polarity) must appear with the same probability everywhere all around the spot and would then show no polarity correspondence with the penumbral neutral line. We must conclude, then, that the polarity distinction seen in the true sign image (*right*) is due to a mostly horizontal magnetic field residing in the moat.

The process that has allowed the detection of the moat filaments is an increase in the signal-to-noise ratio (S/N) of the averaged images by a factor of 25 (from 12 G to better than 1 G). These individual moat filaments are hardly detected in the magnetogram animation (see Fig. 1*b*). Only after their identification in the averaged images can one find some traces of these structures at selected instants of time in the animations.

Canopy fields (as observed by Lites et al. 1993) can only have a minor effect in our averaged signals. The canopy extending into the chromosphere is produced by the vertical component of the penumbra, with typical inclinations of 60°. As the MDI spectral line forms below, say, 400 km above the optical depth unity level in the photosphere, these field lines will never occupy more than two high-resolution MDI pixels beyond the penumbral boundary. The white polarity rim seen in the center side of the true sign image (Fig. 2, *right*, bottom part of the spot), just outside the penumbral boundary, could be produced by these canopy fields. But the signals from the moat filaments in Figure 2 (in particular those marked by the arrows) extend much farther than 2 pixels.

The moat filaments are more conspicuously seen in the structure that is located in the upper part of the spot (marked by the vertical arrow in Fig. 2, *right*). This structure is shown in an expanded view in Figure 3, which uses the same data as in Figure 2. These filaments are seen to begin at coordinates (8″, 12″) as positive polarity filaments (*arrows*). This location corresponds to the mid-penumbra. In the left panel (absolute value of the magnetogram signal), the paths are darkened as they reach the local penumbral neutral line and reappear afterward. They then cross the penumbral outer boundary, continue all over the moat region, and end in two bright patches [coordinates (8″, 30″)]

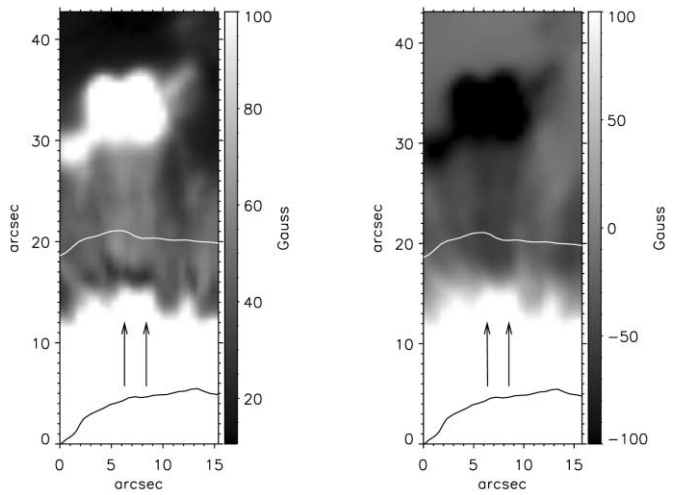

FIG. 3.—Two moat filaments starting inside the penumbra, in absolute value (*left*) and true sign (*right*), extracted from the averaged magnetograms in Fig. 2. [The bottom left corner of these images corresponds to coordinates (83, 106) in Fig. 2.] The arrows indicate where the moat filaments are seen. Scaling is between 0 and 100 G (*left*) and ± 100 G (*right*).

of polarity opposite that of the spot (see Fig. 3, *right*). The moat filaments extend in this case for 12″ beyond the penumbral boundary. Note how the dark gap in the left panel corresponds to the change in polarity as seen in the true sign image (*right*). At this precise location (the neutral line in the filaments), the mean field lines are inclined exactly 80° with respect to the vertical. In the absence of vector magnetic field data, all we can say beyond that point is that the temporally averaged moat filaments found in Figure 3 reach even larger inclinations, although a precise value cannot be given. A vertically oriented weakening of the signal in the middle of the structure seems to indicate the presence of two distinct filaments. However, note that a number of individual (spatially and temporally unresolved) moat filaments may be contributing to these structures. An important point to remark is that the magnetogram signals allow easy traceability from inside the penumbra into the moat, something that was prevented in the Ca II filaments observed by Shine & Title (2001).

We have carefully studied MMFs that occur precisely along the filaments of Figure 3. Four bipolar structures have been detected. One already exists in the moat at the beginning of the lapse. The other three are generated during the time interval studied here. The magnetogram animation marks with arrows all of these MMFs for their clear identification. Figure 4 shows their evolution, from inside the penumbra to the moat. Two properties of these MMFs are worth emphasizing. First, they are all bipolar during their crossing of the moat. In contrast, the filaments in the true sign image of Figure 3 (*right*) are of uniform negative polarity in the moat. But remarkably, what is seen in the animations are strong bipolar structures. Second, these bipolar MMFs are generated as such *inside* the penumbra. The white component of these three MMFs is always identified as beginning well inside the penumbra (of dominant negative polarity in this portion). Table 1 shows information about these three MMFs. The first case is a well-defined white-leading (farthest from the spot) polarity MMF (snapshots 22–144 in the animation). It starts 4″ inside the penumbra and runs until the outer edge of the moat. Note that the white-leading/black-following MMF pair is immediately followed by another white polarity patch. Thus, a clear train of white-black-white can be

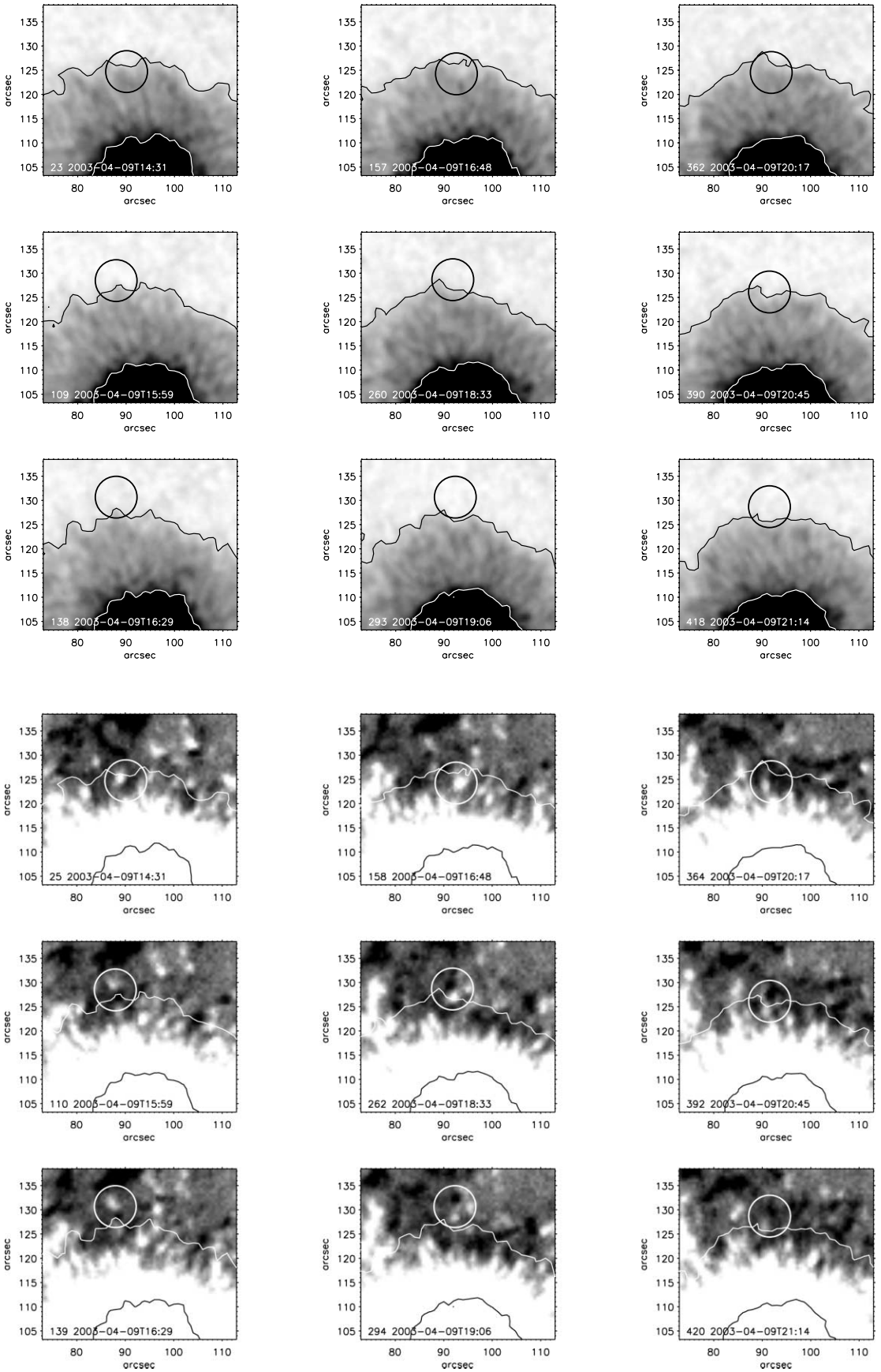

FIG. 4.—*Top*: Continuum intensity images with instantaneous penumbral contours for the three bipolar MMFs detected along the filaments shown in Fig. 3 and starting inside the penumbra. Each column corresponds to a different MMF, where we have marked with a circle three different positions: inside the penumbra, just crossing the penumbral edge, and just after entering the moat. The coordinates correspond with those shown in Fig. 1. Frame number (corresponding to the animation), date, and time are given in the lower-left corner. *Bottom*: Corresponding magnetograms, where the different MMFs can be identified.

TABLE 1
BIPOLAR MOVING MAGNETIC FEATURES STARTING IN THE MID-PENUMBRA

Image No. (1)	Date and Starting Time (2)	Leading Polarity (3)
22.....	2003 Apr 9 14:28	White
159.....	2003 Apr 9 16:49	Black
366.....	2003 Apr 9 20:19	Black

NOTES.—Col. (1): Image number (as shown in the animation). Col. (2): Date and time. Col. (3): Polarity of the leading footpoint MMFs that are created in the mid-penumbra and enter the moat. The sunspot parent polarity is positive.

identified in some snapshots. All three patches form inside the penumbra. This could reflect a sea serpent–like flux tube similar to the model proposed by Harvey & Harvey (1973; but generated inside the spot). The second MMF is a black-leading polarity MMF (snapshots 159–300), but it begins with a white footpoint leading the MMF, 4″ inside the penumbra, that is soon overtaken by the black portion. After that, the black footpoint diffuses temporarily, then reappears, crosses the moat, and merges with the two black polarity patches near the end of the moat (see Fig. 3). One could identify this MMF with two monopolar features, one of the polarity of the spot that moves relatively slow (type II of Shine & Title 2001) and a fast opposite-polarity MMF of type III. Again, all of them are generated inside the penumbra. The white polarity cancels in the middle of the moat with negative flux that keeps emanating from the spot as part of the MMF activity and that moves at faster speeds. The third MMF (snapshots 366–431) comes from 3″ inside the penumbra. It is a black-leading bipolar MMF with a clearly identified white footpoint. Now, the two footpoints seem to cancel themselves in the middle of the moat. Simultaneously, they interact with additional black polarity flux present in the moat. This is, to our knowledge, the first clear evidence of MMFs originating inside the spot (not just somewhere in the moat or at the penumbral boundary; Shine & Title 2001). Note that besides those cases studied here, one can identify in the animation other MMFs starting inside the penumbra in this limb side of the spot.

Additional evidence of the generation of bipolar MMFs inside the penumbra comes from the analysis of what we call the cancellation magnetogram. The cancellation magnetogram is computed by subtracting the absolute value of the true sign average image from the absolute value average image, that is, $\langle|\Phi|\rangle - |\langle\Phi\rangle|$. By definition, the cancellation magnetogram is a positive quantity that depends on the interval of time over which the averages are made. The resulting cancellation magnetogram, for the slightly more than 10 hr analyzed in this work, is shown in Figure 5 (scaled between 0 and 20 G). The information content of this cancellation magnetogram needs some description. First, suppose that one computes this difference at a pixel that, during the averaged interval, is dominated by noise. In this *i*th pixel one would measure $\Phi_i = \epsilon_i$, where ϵ represents a random variable with zero mean (the zero-point level of MDI is well below 1 G; Liu et al. 2004) and standard deviation $\sigma_{\rm MDI}$, the noise level of MDI (around 12 G). When we estimate $\langle\Phi\rangle$ the resulting image fluctuates around zero mean with an rms value of $\sigma_{\rm MDI}/N^{1/2}$, where N is the number of images included in the analysis (633). As pointed out already, this produces a noise level of 0.5 G (i.e., the noise in the true sign average magnetogram). However, when we estimate $\langle|\Phi|\rangle$, the situation is different, as all pixels provide a positive contribution. If we assume that ϵ is normally distributed, it can be shown that the expected value of $\langle|\Phi|\rangle$ is $(2/\pi)^{1/2}\sigma_{\rm MDI}$, around 9 G. Subtracting the absolute value of $\langle\Phi\rangle$ (the 0.5 G mentioned above) from this number becomes negligible, and thus noise-dominated pixels in the cancellation magnetogram typically achieve values near this 9 G level. Now, assume that the pixel is dominated by a constant, large value of the magnetic flux so that the measured number is $\Phi_i = B_i + \epsilon_i$, with $|B_i| > \sigma_{\rm MDI}$. This is the situation for most of the sunspot and strong plage pixels. It is clear that in this case, both averages, $\langle|\Phi|\rangle$ and $|\langle\Phi\rangle|$, have an expected value of B_i (with an uncertainty provided, again, by $\sigma_{\rm MDI}/N^{1/2}$). The subtraction of the two numbers now has an expected value of 0 G. These two cases, noise-dominated areas (*gray areas*, near 9 G) and strong flux regions (*black areas*, near 0 G) are easily seen in Figure 5. Suppose now that a pixel would have, for a portion of the interval under study, a noise-dominated situation and for the rest a given flux level of always the same polarity (as would be produced by the occasional crossing of a unipolar MMF). Clearly, $\langle|\Phi|\rangle - |\langle\Phi\rangle|$ would now be intermediate, somewhere in the interval [0, 9] G. This renders pixels where only unipolar MMFs contribute hardly detectable in Figure 5. Finally, consider the case in which pixels have opposite-polarity signals during the time interval analyzed. If a pixel has, for half of the interval studied, a strong flux $|B_i| > \sigma_{\rm MDI}$, so that the measured value is $+B_i + \epsilon_i$, and for the other half $-B_i + \epsilon_i$, $\langle|\Phi|\rangle$ converges to B_i, but $|\langle\Phi\rangle|$ converges to 0, maximizing the value obtained in the cancellation magnetogram. In Figure 5, the maximum signals attained are ~210 G near plage neutral lines. In the moat, they are typically between 10 and 50 G. In general, for pixels bearing opposite-polarity fluxes during the averaged interval, the cancellation between them in $|\langle\Phi\rangle|$ forces $\langle|\Phi|\rangle \gg |\langle\Phi\rangle|$, producing a signal in the cancellation magnetogram. Note how at the north part of the spot and 4″–5″ inside the penumbra, the corrugated neutral line stands out clearly. Bipolar MMF paths are seen to start there, cross the penumbral boundary, and enter the moat region.[3]

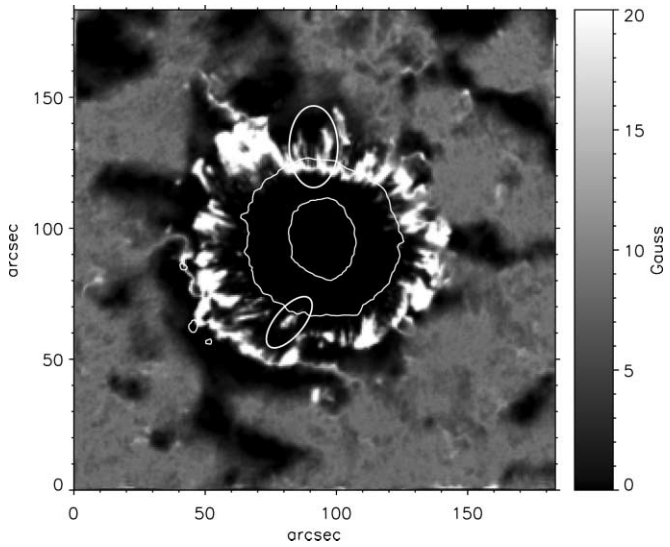

FIG. 5.—Cancellation magnetogram computed by subtracting the absolute value of the true sign average magnetogram (absolute value of Fig. 2, *right*) from the absolute value average magnetogram (Fig. 2, *left*). Scaling is between 0 and 20 G. The ellipses mark bipolar MMFs' paths, discussed in the text. The mean umbral and penumbral contours are indicated.

[3] As already mentioned, one unipolar MMF would give a negligible contribution to the cancellation magnetogram, but two unipolar MMFs following the same path and separated by several hours could provide an important contribution. However, inspection of the magnetogram animation shows that this is not observed in the limb-side moat, where one finds only bipolar activity.

The situation in the other sectors of the spot (corresponding to the center side, dominated by white polarity portions) is different. One of the moat filaments identified in the absolute value average image in Figure 2 (*left arrow*) has a clearly visible bipolar MMF that in this case is seen to start right at the penumbral boundary (Fig. 5, *bottom ellipse*). Other paths are visible, but most of them start somewhere in the middle of the moat region. The southernmost part of the penumbral boundary is seen to be dominated by a dark rim that surrounds this portion of the spot. We want to stress that, as can be seen in the true polarity image in Figure 2 (*right*), this portion is dominated by white polarity fluxes (with contributions from the canopy) that prevent detection of bipolar MMFs starting closer to the spot (or inside the penumbra). Alternatively, bipolar MMFs can appear in the middle of the moat (as shown by Zhang et al. 2003). This can have a correspondence with the bright paths seen in the southern part of the cancellation magnetogram. Note that the MMF "front" where these paths originate can be seen in the true sign average image of Figure 2 (*right*). The polarity of the farthest footpoint of the bipolar MMFs seen here is the same as the polarity of the parent spot, as was found in 85% of the cases studied by Zhang et al. (2003).

4. CONCLUSIONS

SOHO MDI magnetograms, with their constant image quality and sensitivity (both crucial for this investigation), are used to search for evidence that the MMF activity seen surrounding sunspots is magnetically linked to the spot. A more than 10 hr long sequence of high-resolution magnetograms with the symmetric leader sunspot of NOAA AR 0330 has been studied to this end. The time average of the full sequence produces a magnetic flux distribution with two important properties. First, the moat magnetic field found in the true sign averaged image is spatially distributed in agreement with the location of the penumbral neutral line. This neutral line divides the spot in two well-separated polarity regions that are seen to extend into the moat area. The fact that the moat field is separated into these two opposite-polarity regions is interpreted as a predominantly horizontal magnetic field that pervades the moat region. In individual LOS magnetograms, with a much lower S/N than in the averaged image, these horizontal fields are hardly seen, and the moat is dominated by the more transient (and localized) MMF activity. Second, magnetic fields in the moat region are seen to be structured in filaments that can be traced back into the mid-penumbra and that occur everywhere in the moat. Filaments that extend for about $17''$ ($12''$ in the moat and $5''$ inside the penumbra) are seen in the averaged frames. They can be detected in both the limb and center sides of the spot, although they differ in their strength and magnetic polarity (both dominated by projection effects of almost horizontal field lines in LOS magnetograms). The location of the neutral line in the limb-side filaments (Fig. 3) clearly shows that in the moat, the filaments must have inclinations with respect to the vertical larger than 80°. The fact that the filaments can be traced continuously shows that the average inclinations are not much larger than 90°, or else the filaments would be directed back into the Sun. We do not exclude that for some time intervals the filaments are actually forced to reenter below the photosphere. But on average, they must be very close to horizontal, as shown by the continuity from inside the penumbra to the opposite-polarity footpoints.

MMFs are seen in the magnetogram animation, including a permanent magnetic swell all around the spot that follows the polarity distinction set by the penumbral neutral line. We interpret this swell as the temporal fluctuations of the horizontal moat field lines detected in this work. Bipolar MMF activity is seen to be linked to the moat filaments described above. Four bipolar MMFs are seen along the two moat filaments on the limb side of the spot, and one is seen in one of the center-side filaments (Fig. 5, *ellipses*). Three of the limb-side bipolar MMFs are seen to start $4''$–$5''$ inside the penumbra. This has been clearly demonstrated by the sequence shown in Figure 4, the magnetogram animation, and the cancellation magnetogram. It is important to stress here that the merit of this finding is mostly due to the otherwise trivial use of the instantaneous penumbral boundary as a reference all throughout the analysis. If theses boundaries were not displayed in the animations or in the figures, MMFs starting inside the limb-side penumbra would have not been identified.

Another key factor that has played a role in our results is the visibility effects of the center- and limb-side fields in LOS magnetograms. This applies to both the horizontal moat filaments and the MMF activity. As the spot is outside the disk center, one of the sides (the center side) is more aligned with the line of sight and produces the dominant (positive) polarity distribution seen everywhere in the south part of the spot. As explained above, this is also where canopy fields are seen to have a contribution just outside the penumbral boundary. The limb side behaves differently. As we approach the neutral line, the distinctly inclined penumbral components are seen with a different visibility. As we pass the corrugated penumbral neutral line, we find pixels of negative polarity that must have no (or small) contribution from the more vertical component. Thus, these pixels, seen everywhere in the outer limb-side penumbra, must be dominated by the horizontal component (with inclinations larger than 80°). This is the component that is known to carry the ubiquitous Evershed flow and is seen to extend into the moat. In this way, a link between the horizontal moat filaments, bipolar MMFs starting inside the penumbra, and the fate of the Evershed flow is established (although admittedly, we lack direct Doppler shift measurements that would confirm this point).

The results presented in this paper actually fit rather well with current models of both Evershed flow and MMF activity. Schlichenmaier (2002) has shown that the evolution of thin flux tubes, as the Evershed-carrying flow component, can lead to density enhancements that form a serpentine component inside the penumbra. This would correspond with the reported MMF activity starting inside the spot, as found in this paper (this oscillating solution for a siphon flow model was also anticipated by Thomas & Montesinos 1990). Similarly, Weiss et al. (2004) proposed a model in which the downward directed penumbral field lines originate from a flux pumping effect due to the interaction with convection. In this way an explanation for the bipolar MMFs and MMFs with polarity opposite that of the parent spot is provided. These components of the MMF activity would not participate in the sunspot decay process itself and would explain the findings of Martínez Pillet (2002). What is important to remark is that the model proposed by Weiss et al. (2004) predicts the existence of, in an average sense, horizontal moat filaments surrounding the spot, as found in this paper. Monopolar MMFs with the same polarity as the parent spot could still be related to the decay process as traditionally envisaged (Harvey & Harvey 1973).

We conclude, then, that models able to include the Evershed flow in a channeled structure inside the penumbra and its subsequent behavior once the flow leaves the parent spot trunk to interact with the surrounding convective patterns could help in our understanding of MMF activity. From an observational point of view, the efforts should concentrate on the detection of the

horizontal filaments in high sensitive vector magnetograms. Their detection, together with the Doppler signals that would be seen in them, could help solidify the nature of the link between the Evershed flow and MMF activity. The high sensitivity and temporal stability needed for this data make such a study a perfect target for the Japanese-led mission *Solar-B* (to be launched in 2006).

Thanks are due to an anonymous referee, who has helped in clarifying the concepts presented in this paper. Comments on an earlier version of this paper by B. Ruiz Cobo and A. López Ariste are gratefully acknowledged. This research has been funded partly by the Spanish Ministerio de Educación y Ciencia through projects AYA2004-05792 and ESP2003-07735. A. S. D. wants to thank ESA for a grant for attending the IAU Symposium 223.

REFERENCES

Bellot Rubio, L. R. 2003, in ASP Conf. Ser. 307, Solar Polarization, ed. J. Trujillo-Bueno & J. Sanchez Almeida (San Francisco: ASP), 301
Bellot Rubio, L. R., Balthasar, H., & Collados, M. 2004, A&A, 427, 319
del Toro Iniesta, J. C., Bellot Rubio, L. R., & Collados, M. 2001, ApJ, 549, L139
Harvey, K., & Harvey, J., 1973, Sol. Phys., 28, 61
Lee, J. W. 1992, Sol. Phys., 139, 267
Lites, B. W., Elmore, D. F., Seagraves, P., & Skumanich, A. P. 1993, ApJ, 418, 928
Liu, Y., Zhao, X., & Hoeksema, T. 2004, Sol. Phys., 219, 39
Martínez Pillet, V. 1997, in ASP Conf. Ser. 118, First Advances in Solar Physics Euroconference: Advances in Physics of Sunspots, ed. B. Schmieder, J. C. del Toro Iniesta, & M. Vázquez (San Francisco: ASP), 212
———. 2002, Astron. Nachr., 323, 342
Meyer, F., Schmidt, H. U., Wilson, P. R., & Weiss, N. O. 1974, MNRAS, 169, 35
Scherrer, P. H., et al. 1995, Sol. Phys., 162, 129
Schlichenmaier, R. 2002, Astron. Nachr., 323, 303
Schlichenmaier, R., & Schmidt, W. 2000, A&A, 358, 1122
Sheeley, N. R. 1969, Sol. Phys., 9, 347
Shine, R., & Title, A. 2001, in Encyclopedia of Astronomy and Astrophysics, Vol. 4, ed. P. Murdin (London: Nature Publishing; and Bristol: IOP Publishing), 3209
Solanki, S. K. 2003, A&A Rev., 11, 153
Solanki, S. K., & Montavon, C. A. P. 1993, A&A, 275, 283
Thomas, J. H., & Montesinos, B. 1990, ApJ, 359, 550
Thomas, J. H., & Weiss, N. O. 2004, ARA&A, 42, 517
Thomas, J. H., Weiss, N. O., Tobias, S. M., & Brummell, N. H. 2002, Astron. Nachr., 323, 383
Title, A. M., Frank, Z. A., Shine, R. A., Tarbell, T. D., Topka, K. P., Scharmer, G., & Schmidt, W. 1993, ApJ, 403, 780
Weiss, N. O., Thomas, J. H., Brummell, N. H., & Tobias, S. M. 2004, ApJ, 600, 1073
Westendorp Plaza, C., del Toro Iniesta, J. C., Ruiz Cobo, B., Martínez Pillet, V., Lites, B. W., & Skumanich, A. 1997, Nature, 389, 47
Zhang, J., Solanki, S. K., & Wang, J. 2003, A&A, 399, 755